

Fully Quantum Rovibrational Calculation of the He(H₂) Bound and Resonance States[†]

Yingsheng Xiao and Bill Poirier*

Department of Chemistry and Biochemistry, and Department of Physics, Texas Tech University, Box 41061, Lubbock, Texas 79409-1061

Received: October 31, 2005

In a recent paper [*J. Chem. Phys.* **2005**, *122*, 124318], a full-dimensional quantum method, designed to efficiently compute the rovibrational states of triatomic systems with long-range interactions, was applied to the benchmark Li⁻(H₂) ion–molecule system. The method incorporates several key features in order to accurately represent the rovibrational Hamiltonian using only modestly sized basis sets: (1) exact analytical treatment of Coriolis coupling; (2) a single bend-angle basis for all rotational states; (3) phase space optimization of the vibrational basis; (4) G₄ symmetry adaptation of the rovibrational basis. In this paper, the same methodology is applied for the first time to a van der Waals complex system, He(H₂). As in the Li⁻(H₂) study, all of the rovibrational bound states, and a number of resonance states, are computed to very high accuracy (¹/_{10 000} of a wavenumber or better). Three different isotopologues are considered, all of which are found to have a single bound state with a very low binding energy. Several extremely long-lived Feshbach resonances are also reported.

I. Introduction

The He(H₂) system has been studied theoretically for decades.^{1–4} It is of great interest for quantum chemistry, serving as the simplest test case for theories of the interactions of a molecule with a closed-shell atom. This system is also of particular interest in astrophysics, in that helium and hydrogen compose the giant molecular clouds of the interstellar medium.³ Heating of these clouds by strong shock waves causes rotational and vibrational excitation of the H₂ molecules and can lead to collision-induced dissociation of H₂ into free H atoms. Because of the extremely low density of the clouds (mean free molecular paths of thousands of kilometers), these processes cannot be readily studied experimentally, thus motivating theoretical investigations, particularly at low energies/temperatures. In broader terms, the He(H₂) system is also interesting from the standpoint of being a van der Waals (vdW) complex. In particular, the predissociation of vdW complexes has been a topic of long-standing theoretical and experimental investigation.^{5–8} Initial studies were motivated by the desire to unveil how bulk properties of materials emerge from those of smaller systems.^{9,10} These have subsequently come to serve as prototypes for other important phenomena such as solvation.

Recently, high-accuracy theoretical calculations for vdW complex formation have been further motivated by a novel idea: creating ultracold molecules for a number of important applications, such as the formation of molecular Bose–Einstein condensates (BECs), the production of molecular lasers (i.e., coherent beams of state-selected molecules), and so forth. Most of the methods for producing cold molecules create species that are translationally cold but internally excited (electronically, vibrationally, or rotationally). Understanding the rates of collision processes involving cold and ultra cold molecules is thus crucial for guiding new experimental developments. Since the collision rates can be difficult to measure experimentally, there

is a desire to obtain these from theoretical calculations, e.g., the pioneering studies by Dalgarno and co-workers.^{11,12}

In the case of He(H₂), the well depth is so shallow ($D_e = 10.3 \text{ cm}^{-1}$),¹³ and the masses so light, that there has been a question as to whether bound states even exist. In a recent experiment by Kalinin and co-workers,¹⁴ the presence of a bound He(H₂) complex was identified in a molecular beam produced by cryogenic free jet expansion of a mixture of H₂ and ⁴He gases (1% H₂ in 99% ⁴He). The experiment measured the first-order diffraction angle after passing a molecular beam through a 100-nm-period transmission grating. Although this work provides strong evidence for the existence of a bound ⁴He(H₂) complex, the extremely small observed binding energy, D_0 , was too small to be determined accurately but could only be estimated as being less than around 0.04 K ($\sim 0.03 \text{ cm}^{-1}$). Similarly, although potential features of the He(H₂) system have been investigated for many years (for a review, see the introduction of ref 13), only recently has a global potential energy surface (PES) been developed (by Boothroyd and co-workers¹³) that may be sufficiently accurate to theoretically establish the existence of bound He(H₂) rovibrational states.

Using the PES of Boothroyd et al., Gianturco et al. computed a single rovibrational bound state for He(H₂), with an extremely small binding energy of $D_0 = 0.03634 \text{ cm}^{-1}$.¹⁵ Resonance states were not considered. Using a different and less accurate PES,⁴ Balakrishnan, Forrey, and Dalgarno conducted a theoretical calculation of ultracold atom (He) and diatom (H₂) scattering,¹¹ which also predicted the existence of a bound He(H₂) complex ($D_0 = 0.0298 \text{ cm}^{-1}$), together with a set of Feshbach resonance states (some of which are extremely long-lived) corresponding to vibrationally excited H₂. Using empirical diatomic pair interaction potentials and ignoring three-body interactions, Li and Lin¹⁶ also predicted a bound state with an estimated D_0 of 0.0474 cm^{-1} .

Although fully quantum vibrational ($J = 0$) calculations for covalently bonded triatomic systems (at reasonably low energies) have become fairly routine, rovibrational calculations for vdW

[†] Part of the special issue "John C. Light Festschrift".

* Email: Bill.Poirier@ttu.edu.

triatomic systems still pose a major computational challenge. This is because the long-range vdW interactions require a far greater range of stretch coordinate values, i.e., typically several hundred atomic units, or 2–3 orders of magnitude larger than for typical covalent bonds. This results in a calculation that requires far more basis functions or grid points. In the He(H₂) case, in particular, although there is evidently only one bound state, the close proximity to the dissociation threshold ensures that the wave function even for this ground vibrational state will have a very long tail. Moreover, the extremely small D_0 value also implies that a very highly accurate calculation must be performed in order to compute this quantity to a reasonable level of relative accuracy. For the rovibrational calculations (required here to establish the nonexistence of $J > 0$ bound and resonance states), the computational effort is correspondingly greater, owing to the $(2J + 1)$ different values for the rotational quantum number K .

In a previous paper,⁸ a combination of computational methods was suggested as being particularly effective for performing exact quantum calculations of the rovibrational states of triatomic vdW and ion–molecule systems. The method treats Coriolis coupling exactly and analytically.¹⁷ Moreover, through a different partitioning of the various rovibrational kinetic energy terms than is standard, the full rovibrational Hamiltonian may be represented exactly using a true direct-product basis representation. In particular, the same bend-angle basis set may be used for all rotational-state J and K values and for the off-diagonal Coriolis coupling blocks ($K \neq K'$). This is achieved by representing part of the kinetic energy as a three-body “centrifugal potential”, which is added to the true potential, and represented using the same quadrature scheme.^{17,18} The vibrational basis set/quadrature scheme is obtained using the phase space optimized discrete variable representation (PSO DVR) method,^{8,19–22} which is particularly well-suited to long-range potentials, vis-à-vis reducing the total size of the vibrational Hamiltonian matrix. Further reduction in matrix size is achieved using G_4 symmetry adaptation of the rovibrational basis.⁸

In ref 8, the above scheme was applied to the Li[−](H₂) ion–molecule system and found to be remarkably efficient. Indeed, the matrices required to compute all bound rovibrational states to an accuracy of 0.005 cm^{−1} or better were sufficiently small to be stored and directly diagonalized on a single CPU (i.e., without exploiting sparsity). A number of rovibrational resonance states were also computed, including some unexpected very long-lived (sub-milliseconds) Feshbach resonances, associated with internal relaxation of the bending mode. This confirmed a previous classical model prediction by Beswick and collaborators^{5–7} that weakly interacting complexes can support extremely long-lived rovibrational predissociation states. Among other reasons for being of interest, Feshbach resonances play a very crucial role in producing molecular BECs²³ (section 4).

The present paper represents the first application of the above methodology to a vdW complex system. In particular, we address the existence or nonexistence of $J = 0$ and $J > 0$ rovibrational bound states for He(H₂) and perform a highly accurate calculation of the binding energy, D_0 , for comparison with previous theoretical calculations. We also calculate the rovibrational resonances, computing energies, widths, and lifetimes, with a special emphasis placed on the Feshbach resonance states. Finally, the role of isotopic substitution is considered, both for the He atom and for one of the two H atoms.

II. Theory and Computational Details

For the most part, the theory and methodology used in this paper have been described in previous publications.^{8,17–22} Accordingly, here we provide only a summary of the methodology, as well as computational details pertinent to this specific He(H₂) vdW complex system.

A. Coordinates and Potential Energy Surface. Jacobi vectors \mathbf{r} and \mathbf{R} (space-fixed) are used to define the rovibrational coordinate system, with the vector \mathbf{r} representing the H–H separation and \mathbf{R} the separation between the He atom and the H₂ center of mass. The corresponding reduced masses are m and M , respectively. The body-fixed frame is defined using the standard “ r -embedding”²⁴ or “ z z gauge”,²⁵ i.e., the body-fixed z axis points along the vector \mathbf{R} , and the angle formed by \mathbf{r} and \mathbf{R} defines the body-fixed x – z plane. The magnitude of this bend angle, γ , together with the vector lengths, r and R , compose the vibrational coordinates.

For the He(H₂) PES, we used the highly accurate global surface developed recently by Boothroyd et al.¹³ This analytic PES, with 112 parameters, was fit to a large number of ab initio energies (more than 20 000). The ab initio energy calculations have an estimated root mean square (rms) “random” error of 0.2 millihartree. However, the fitting procedure uses a reduced weight for the high-energy ab initio points, in order to more accurately reflect the interaction region. The Boothroyd et al. PES exhibits a slightly bent equilibrium geometry, with $\gamma_{\text{eq}} = 19.2^\circ$. The equilibrium H–H separation, r_{eq} , is close to that of an isolated H₂ molecule, whereas the equilibrium He–H₂ separation, R_{eq} , is fairly large (about 6.3 au). Even by the standards of vdW complexes, the well depth (classical dissociation energy) $D_e = 10.3$ cm^{−1} is quite shallow.

B. Basis Representation of the $J = 0$ Hamiltonian Matrix. For the vibrational ($J = 0$) Hamiltonian, \hat{H}_{00} , the standard differential form in terms of (R, r, γ) is applicable, i.e.

$$\hat{H}_{00} = -\frac{\hbar^2}{2MR^2} \frac{\partial}{\partial R} R^2 \frac{\partial}{\partial R} - \frac{\hbar^2}{2mr^2} \frac{\partial}{\partial r} r^2 \frac{\partial}{\partial r} - \left(\frac{\hbar^2}{2MR^2} + \frac{\hbar^2}{2mr^2} \right) \left(\frac{1}{\sin \gamma} \frac{\partial}{\partial \gamma} \sin \gamma \frac{\partial}{\partial \gamma} \right) + V(R, r, \gamma) \quad (1)$$

Two types of DVRs^{26–32} were employed for the vibrational basis representation. In particular, PSO DVRs^{8,19–22} were used for r and γ , wherein marginal effective potentials, $V_r(r)$ and $V_\gamma(\gamma)$, were customized for the eq 1 vibrational Hamiltonian. For the present application, $V_r(r)$ and $V_\gamma(\gamma)$ were computed at a large number (~ 5000) of uniformly spaced points in their respective coordinates, r and γ . Cubic spline interpolation³³ was then used to compute these functions at arbitrary coordinate values. The density of points is sufficiently large to eliminate numerical problems such as spline-ringing, known to adversely affect DVR techniques.^{20,32}

Initially, a PSO DVR in R was also used, in conjunction with a rescaling technique³⁴ that reduces quadrature error at the expense of increased basis set error. However, convergence difficulties for the γ -excited resonance states prompted a switch to the more straightforward (but less efficient) uniformly spaced sinc-DVR basis²⁹ for the coordinate R . The convergence difficulties remained (section 3.2), but the sinc-DVR basis was nevertheless retained. Even with this choice, the largest matrices required were still found to be sufficiently small to allow for direct diagonalization on a single CPU, without exploiting sparsity.

C. Basis Representation of the $J > 0$ Hamiltonian Matrices. Once the $J = 0$ vibrational Hamiltonian matrix, \hat{H}_{00} ,

is determined, it is straightforward to obtain the exact rovibrational Hamiltonian matrix for any $J > 0$ value, using the method described in section 1.¹⁷ With the standard Wigner rotation functions³⁵ as the rotational basis, $|JKM\rangle$, the resultant $J > 0$ matrix is essentially independent of M ($M = 0$ chosen for convenience) and block tridiagonal in K . Regarding each rotational block as a differential operator acting on the internal coordinates, (R, r, γ) , these blocks can be given explicitly as follows:^{17,18}

$$\begin{aligned}\hat{H}_{JK} &= \langle JKM|\hat{H}|JKM\rangle \\ &= \hat{H}_{00} + \frac{\hbar^2 J(J+1)}{2MR^2} + \left(\frac{1}{2mr^2 \sin^2 \gamma} + \frac{\cot^2 \gamma - 1}{2MR^2} \right) \hbar^2 K^2\end{aligned}\quad (2)$$

$$\begin{aligned}\hat{H}_{JK\pm} &= \langle J(K\pm 1)M|\hat{H}|JKM\rangle \\ &= \frac{\hbar^2}{2MR^2} \sqrt{J(J+1) - K(K\pm 1)} \left(\mp \frac{\partial}{\partial \gamma} + K \cot \gamma \right)\end{aligned}\quad (3)$$

The last two terms in eq 2 above may be regarded as a J - and K -dependent three-body “centrifugal potential” contribution, which can be easily represented as a diagonal matrix, using the vibrational DVR quadrature scheme of section 2.2. To compute the diagonal blocks, \hat{H}_{JK} , this diagonal centrifugal potential matrix is simply added to the vibrational \hat{H}_{00} matrix discussed previously.

The off-diagonal blocks, $\hat{H}_{JK\pm}$, represent Coriolis coupling. Note that this contribution involves a partial derivative in γ . Instead of obtaining the corresponding γ matrix elements numerically via quadrature integration on the γ grid, one can obtain a completely analytical characterization of this contribution in the standard (i.e., *not* associated) Legendre polynomial representation using a recent method.¹⁷ Straightforward transformations can then be used to obtain the corresponding γ PSO DVR representation. Since only *one* bend-angle basis set need be considered for *all* J and K values, the matrix elements for eq 3 need only be evaluated once.

D. Symmetry Adaptation of the $J > 0$ Hamiltonian Matrices. To further reduce the $J > 0$ Hamiltonian matrix sizes, a symmetry adaptation scheme was applied to the rovibrational basis set, according to the G_4 permutation inversion (PI) group. There are four irreducible representations (irreps) for this group: A^+ , A^- , B^+ , B^- , with A/B denoting permutation symmetry (H atom exchange) and \pm denoting overall parity (space-fixed inversion). Note that the above symmetry labels refer to the full six-dimensional (6D) rovibrational wave function. The corresponding 6D basis functions are denoted $|JKM\rangle|\gamma_\alpha r_\beta R_\gamma\rangle$, where $|\gamma_\alpha\rangle$, $|r_\beta\rangle$, and $|R_\gamma\rangle$ are the one-dimensional (1D) vibrational DVR basis functions in the respective angular and radial coordinate spaces.

The symmetry-adapted basis functions were constructed from the 6D basis functions described above by applying the four G_4 irrep projection operators. The resultant symmetry-adapted linear combinations are presented in eq 4. Note that, since the G_4 symmetry operations affect only $|K\rangle$ and $|\gamma_\alpha\rangle$, the notation $|K\gamma\rangle$ is used in eq 4 as a shorthand for $|JKM\rangle|\gamma_\alpha r_\beta R_\gamma\rangle$.

$$\begin{aligned}|K\gamma\rangle^{A^+} &\propto [|K\gamma\rangle + (-1)^J|(-K)(\pi - \gamma)\rangle + \\ &\quad (-1)^{J+K}|(-K)\gamma\rangle + (-1)^K|K(\pi - \gamma)\rangle] \\ |K\gamma\rangle^{A^-} &\propto [|K\gamma\rangle + (-1)^J|(-K)(\pi - \gamma)\rangle - \\ &\quad (-1)^{J+K}|(-K)\gamma\rangle - (-1)^K|K(\pi - \gamma)\rangle]\end{aligned}$$

$$\begin{aligned}|K\gamma\rangle^{B^+} &\propto [|K\gamma\rangle - (-1)^J|(-K)(\pi - \gamma)\rangle + \\ &\quad (-1)^{J+K}|(-K)\gamma\rangle - (-1)^K|K(\pi - \gamma)\rangle] \\ |K\gamma\rangle^{B^-} &\propto [|K\gamma\rangle - (-1)^J|(-K)(\pi - \gamma)\rangle - \\ &\quad (-1)^{J+K}|(-K)\gamma\rangle + (-1)^K|K(\pi - \gamma)\rangle]\end{aligned}\quad (4)$$

Use of the symmetry-adapted, eq 4 basis, rather than the original $|K\gamma\rangle$ basis, reduces each rovibrational Hamiltonian to four independent diagonal blocks of substantially smaller size. Further details may be found in ref 8

III. Results and Discussion

A. Bound State. Using the methodology described in section 2, only one rovibrational bound state was obtained for the ⁴-He(H₂) system. This state corresponds to p -H₂ (where p stands for “para”), $J = 0$, and the totally symmetric irrep A^+ . No other bound states were computed for the $J > 0$ case, and none were obtained for He(*o*-H₂) (with *o* = “ortho”). The computed binding energy was found to be $D_0 = 0.036\,40\text{ cm}^{-1}$, converged to the last digit indicated, using 1D basis sizes $N_r = 3$, $N_R = 251$, and $N_\gamma = 10$. Other parameters used in the calculation are as indicated in Tables 1 and 2.

Since the r and R motions are very weakly coupled, and the H₂ stretch frequency is so much larger than that of the other vibrational modes (~ 400 times larger than D_e), only a very small number of PSO DVR points in r are required to achieve convergence of the bound-state energy level. In fact, one can further reduce N_r by converging the binding energy (difference between the level energy and the dissociation limit) rather than the level energy itself. The idea is to obtain the dissociation limit numerically, by computing the zero-point energy of (p -H₂) using the same PSO DVR basis in r as is used for the full vdW calculation. Such a scheme is appropriate, given the extremely close proximity of the ⁴He(H₂) bound state to the dissociation limit, and in fact enables D_0 to be converged to around 10^{-5} cm^{-1} .

As discussed in section 1, the well depth (D_e) of the Boothroyd et al. PES for He(H₂) is only about 10.3 cm^{-1} ;¹³ consequently, the existence of a bound level has been in doubt for some time. Considering the extreme closeness of the purported bound level to the dissociation limit (several hundredths of a wavenumber), the existence of such a state is extremely difficult to verify. Our calculation is sufficiently accurate to prove that the Boothroyd PES does indeed support such a state and to determine D_0 to several significant figures. The accuracy of the PES itself (section 2.1) is probably sufficient to confirm the existence of the bound state, but perhaps insufficient for placing much quantitative confidence in the computed D_0 value.

It is instructive to compare the present He(H₂) results with those of the Li⁻(H₂) ion–molecule system.⁸ As is typical for such complex systems, the well depths are both quite small, despite which the ground-state vibrational energy is located most of the way out of the well—i.e., (D_0/D_e) ratios are also quite small. However, this effect is *much* more pronounced in He-(H₂). Another key difference is that D_0 is larger for Li⁻(*o*-H₂) than for Li⁻(*p*-H₂), whereas He(*o*-H₂) is not even found to have a bound state.

Rovibrational bound states were also computed for two additional systems, ³He(H₂) and ⁴He(HD), related to ⁴He(H₂) via isotopic substitution. The same effective potentials were used as for the ⁴He(H₂) calculation; however, the substantially different reduced masses (derived from the Table 1 mass values)

TABLE 1: Masses and Coordinate Ranges Used to Generate Vibrational Coordinate 1D DVR Basis Sets for He(H₂) Calculation^a

category	parameter	value (a.u.)
masses	H	1837.362216
	D	3671.479690
	³ He	5497.886346
	⁴ He	7296.293435
coordinate ranges	r_{\min}	0.6
	r_{\max}	4.0
	γ_{\min}	0.0
	γ_{\max}	π
	R_{\min}	4.0
	R_{\max}	see Table 2

^a All units are atomic units.**TABLE 2: Parameter Values Required to Converge the Various He(H₂) Rovibrational State Calculations^a**

parameter	⁴ He(H ₂) (bound)	⁴ He(H ₂) (resonance with $j = 0$)	⁴ He(H ₂) (resonance with $j > 0$)	³ He(H ₂) (bound)	⁴ He(HD) (bound)
N_r	3	5	3	3	3
N_R	251	240	800	336	251
N_γ	10	10	10	10	10
R_0 (a.u.)		400.0	1600.0		
R_{\max} (a.u.)	216.0	1200.0	8000.0	288.0	216.0

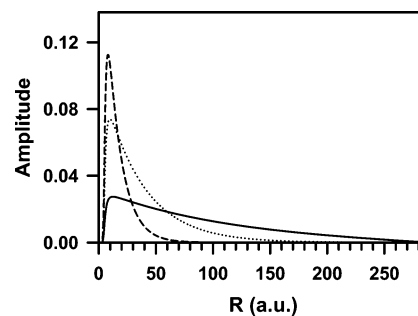
^a The $j > 0$ resonance calculation (column 4) is particularly difficult to converge.**TABLE 3: Computed Binding Energies, D_0 , for Different Isotopologues of the He(H₂) System^a**

isotopologue	D_0		D_0	
	(this work)	(Gianturco et al.)	(Balakrishnan et al.)	(Li et al.)
⁴ He(<i>p</i> -H ₂)	0.03640	0.03634	0.0298	0.0474
³ He(<i>p</i> -H ₂)	0.00327	0.02916	0.0016	0.0072
⁴ He(HD)	0.23089	0.23427		

^a All energies are in cm⁻¹. Column 2 is from this work, while columns 3, 4, and 5 are from Gianturco et al.,¹⁵ Balakrishnan et al.,¹¹ and Li et al.,¹⁶ respectively.

resulted in different PSO DVR vibrational basis sets. The ⁴He(HD) calculation was converged using the same basis sizes as for ⁴He(H₂); however, the ³He(H₂) calculation required a substantially larger R coordinate range and basis size (Table 2). For each isotopic substitution, only a single rovibrational bound state was obtained, corresponding to the same symmetry and quantum number labeling as the ⁴He(H₂) bound state (note: the ⁴He(HD) case uses only G₂ symmetry adaptation and labeling).

The computed D_0 values for all three systems are presented in Table 3 and also compared with previous calculations performed by other researchers. For the two systems involving ⁴He, our results agree very well with a recent calculation by Gianturco et al.,¹⁵ who used the same Boothroyd et al. PES as we did. In particular, both calculations predict nearly an order-of-magnitude increase in D_0 for the HD versus H₂ systems, as is reasonable given the substantially heavier masses involved. Regarding ³He(H₂), the existence of a bound state is even more tenuous than for ⁴He(H₂); our calculations nevertheless unambiguously predict such a state, with $D_0 = 0.003\,27\text{ cm}^{-1}$. This D_0 is roughly an order of magnitude smaller than the ⁴He(H₂) value and disagrees markedly with the Gianturco result, which is only slightly smaller than for ⁴He(H₂). Given the quantitative level of agreement between the two calculations for the other

**Figure 1.** Slice of computed bound state vibrational wave function for different isotopologues of the He(*p*-H₂) system: ⁴He(*p*-H₂) (dotted line); ³He(*p*-H₂) (solid line); ⁴He(HD) (dashed line).

two isotopologues, the reason for the ³He(H₂) discrepancy was initially unclear; however, one possible explanation is provided below.

Balakrishnan, Forrey, and Dalgarno¹¹ also computed D_0 values for the ⁴He(H₂) and ³He(H₂) systems, albeit using a different PES.⁴ Their results are qualitatively similar to ours and, in particular, also exhibit the large D_0 reduction under He isotopic substitution. Similar comments apply to the work of Li and Lin,¹⁶ who used a somewhat less accurate empirical two-body interaction potential. For both systems considered, our computed D_0 values lie between those of Balakrishnan et al. and Li et al.

In addition to computing D_0 values, we have also obtained ground-state vibrational wave functions for each of the three isotopologues considered. These are presented in Figure 1, which are “slices” in R , taken from the 3D computed vibrational wave functions by fixing r and γ near their equilibrium values. Since excitations in r and γ require energies much larger than D_e , the long-range tails evident in the Figure 1 plots provide an indication of the “size” of the bound He(H₂) complexes. This clearly shows a very strong correlation with the reduced mass M . In particular, ⁴He(HD) is much more localized in the vdW well than is ⁴He(H₂), which in turn is substantially more localized than ³He(H₂).

Indeed, from the bound-state wave function plot for ³He(H₂), it is evident why such a large $R_{\max} = 288\text{ au}$ value (Table 2) was required to achieve convergence for this system. In the corresponding Gianturco et al. calculation, the value $R_{\max} = 226.8\text{ au}$ was used, which, on the basis of Figure 1, does not appear to be sufficiently large to adequately capture the long-range tail behavior. This may well account for the observed discrepancy in the computed values for D_0 .

B. Resonance States. Calculations of the rovibrational resonance states were also conducted for the ⁴He(*p*-H₂) system. This was achieved using the methodology of section 2, with the addition of a complex absorbing potential (CAP),^{36–41} $-iW$, along the dissociation coordinate R . A quartic CAP function was employed, i.e.,

$$W(R) = A\Theta[R - R_0] \left(\frac{R - R_0}{R_{\max} - R_0} \right)^4 \quad (5)$$

where $\Theta[]$ represents the step function, R_0 is the point at which the CAP is “turned on”, R_{\max} is the maximum value of the R coordinate grid, and A is the strength parameter. In general, resonance-state calculations are much more difficult than bound-state calculations, because the matrices are complex, rather than real-valued, and the CAP requires a substantially larger R coordinate range. These difficulties are particularly compounded when the relative translational energy of the dissociation

TABLE 4: Computed Resonance Data for the ⁴He(*p*-H₂) System^a

<i>v</i>	<i>j</i>	Δ <i>E</i>	width	lifetime
0	0	-0.03640	0	∞
1	0	-0.04375	2.0 × 10 ⁻¹¹	2.7 × 10 ⁻¹
2	0	-0.04919	2.4 × 10 ⁻¹⁰	2.2 × 10 ⁻²
0	2	-0.058 (±0.014)	<~5 × 10 ⁻⁵	>~1 × 10 ⁻⁷
0	4	-0.062 (±0.013)	<~1 × 10 ⁻⁴	>~5 × 10 ⁻⁸
0	6	-0.068 (±0.017)	<~2 × 10 ⁻⁴	>~3 × 10 ⁻⁸

^a Energies and widths are in cm⁻¹ and lifetimes in seconds. Energies are relative to asymptotically correlating H₂(*v*, *j*) levels.

fragments is small or encompasses multiple scales, as is often the case for vdW complex dissociation. Indeed, the authors are aware of only one other research group (Dalgarno and co-workers)^{11,42} who have addressed the rovibrational resonance states of ⁴He(*p*-H₂).

Our initial resonance calculation was for the *J* = 0 case. Similar to our previous work on Li⁻(H₂), several long-lived Feshbach resonances were observed. However, in the present case, these correspond to excitations in *r* (the H₂ stretch mode) rather than *γ* (the bend mode). In other words, the ⁴He(*p*-H₂) Feshbach resonances correlate asymptotically to H₂(*v*, *j* = 0), with (*v*, *j*) the vibrational and rotational quantum numbers for the H₂ fragment. Another key difference is that the Feshbach resonance lifetimes for ⁴He(*p*-H₂) are much longer than for Li⁻(H₂), i.e., *subseconds*, rather than *sub-milliseconds*. As indicated in (Table 4), these lifetimes are *extremely* long, i.e., for most intents and purposes, these may be regarded as *r* vibrationally excited bound states. It is therefore natural to report these resonance energies relative to the asymptotically correlating He + H₂(*v*) energy levels, as is done in Table 4. In all cases, the relative energies are negative, by a few hundredths of a wavenumber, i.e., the same order of magnitude as *D*₀. The present results agree qualitatively with a previous calculation by Forrey and Dalgarno⁴² using a different PES; in particular, the resonance widths/lifetimes are within an order of magnitude of the ref 42 results.

To converge the above-mentioned Feshbach resonance states to within 5 × 10⁻⁵ cm⁻¹, the parameters listed in Table 2 column 3 were required (also *A* = 1.8 cm⁻¹). In comparison with the bound-state calculation, the primary difference is the increased basis size in *r* (*N_r*), as is to be expected. A much larger *R* coordinate range was also required, in order to accommodate the CAP, although this did not result in a substantially different *N_R* value.

The above calculation also revealed several additional states in the continuum that may correspond to Feshbach resonances with *γ* (or *j*) excitations. These states are indicated by imaginary eigenvalue components³⁶⁻⁴¹ about 2 orders of magnitude smaller than for nearby continuum states. Subsequent detailed convergence studies have shown that these states are *much* more difficult to converge than the *j* = 0 resonances (Table 2, column 4), despite the fact that *N_r* is 60% smaller. In particular, an exceedingly large *R* coordinate range is required, even when a more efficient CAP⁴⁰ is employed.

Our best estimates for the energies, widths, and lifetimes for these *j* > 0 resonances are presented in Table 4. These results were achieved by exploiting the observation that a small set of resonance-like continuum states (identified using the criterion described above) are always found within a small energy “window”, located a few hundredths of a wavenumber below each asymptotic He + H₂(*v* = 0, *j*) energy level. The size of these energy windows decreases with increasing *R*_{max} so that, by extending the *R* coordinate range to *R*_{max} = 8000 au, we

were able to obtain the estimates provided in the last three rows of Table 4. Note that the explicit uncertainties listed in the table refer to the energy window sizes; if a given resonance state exists, it should therefore be located within the corresponding energy window. A quantitative estimate for the width/lifetime of these resonances is difficult to obtain, but it is clear that these are less long-lived than the *j* = 0 resonances by many orders of magnitude. Under the assumption that these resonance-like states correspond to *j* > 0 Feshbach resonances, the computed resonance quantities are indeed in good agreement with the previous work of Forrey and Dalgarno.⁴²

Calculations similar to those described above for *J* = 0 were also performed for the *J* > 0 case. However, no resonances (or resonance-like continuum states) of either variety were observed.

IV. Summary and Conclusions

We have computed all of the rovibrational bound states of ⁴He(H₂), ³He(H₂), and ⁴He(HD) to an accuracy of 1/10,000 of a wavenumber or better. Despite the broad variation in isotopic masses, each of these systems exhibits just a single rovibrational bound state, albeit with vastly varying computed *D*₀ values (~70-fold increase from lightest to heaviest system). In all cases, *D*₀ values are extremely small, even relative to *D_e*. The current *D*₀ results are in qualitative agreement with previous calculations of the He(H₂) bound state, except for the ³He(H₂) *D*₀ value as computed by Gianturco et al.¹⁵ However, analysis of the ground-state vibrational wave function suggests that the previous calculation may be insufficiently converged with respect to the dissociation coordinate range.

Several rovibrational resonance states for ⁴He(H₂) were also computed, although all of these were found to be vibrational (*J* = 0) states. Two distinct categories of resonances emerged, i.e., *j* = 0 versus *j* > 0. The former were found to be extremely long-lived (subsecond) Feshbach resonances. These calculations were relatively easy to converge to a very high level of accuracy, i.e., 1/10,000 of a wavenumber or better. The existence of these *j* = 0 Feshbach resonances thus provides further evidence that weakly interacting complexes can support extremely long-lived vibrational predissociation states. In contrast, the *j* > 0 resonances were found to have lifetimes many orders of magnitude shorter, probably owing to greater coupling between the bend and He stretch modes than between the H–H and He stretch modes. These states were also much more difficult to converge with respect to *R*.

Highly accurate rovibrational calculations of Feshbach resonances for ion–molecule and vdW complexes are exceedingly difficult to perform. These are nevertheless very important, as Feshbach resonances play a crucial role in producing molecular BECs. Recent work by Wieman and co-workers,²³ for example, has shown that an atomic BEC may be partially converted into molecules by magnetic tuning close to a Feshbach resonance. The methodology as applied here for the prototype vdW complex system He(H₂), and in ref 8 for the prototype ion–molecule system Li⁻(H₂), appears to be very successful in meeting this challenge, i.e., in both cases, direct diagonalization on a single CPU was all that was required to obtain highly accurately converged results. We believe that our method would also be effective, more generally, in dynamical studies of ultracold molecules characterized by the extension of vibrational motion up to hundreds or thousands of atomic units.

Acknowledgment. This work was largely supported by the Office of Advanced Scientific Computing Research, Mathematical, Information, and Computational Sciences Division of the

U. S. Department of Energy, under contract DE-FG03-02ER25534. Acknowledgment is also made to The Welch Foundation (D-1523). The authors also wish to express gratitude to Joel Bowman, Tucker Carrington, Jr., Gregory Gellene, William Hase, Michael Minkoff, Edward Quitevis, Pierre-Nicholas Roy, and Albert Wagner, for many stimulating discussions. This paper is dedicated to John C. Light.

References and Notes

- (1) Karplus, M.; Kolker, H. J. *J. Chem. Phys.* **1964**, *41*, 3955.
- (2) Gordon, M. D.; Secrest, D. *J. Chem. Phys.* **1970**, *52*, 120.
- (3) Dove, J. E.; Rusk, A. C. M.; Cribb, P. H.; Martin, P. G. *Astrophys. J.* **1987**, *318*, 379.
- (4) Muchnick, P.; Russek, A. *J. Chem. Phys.* **1994**, *100*, 4336.
- (5) Beswick, J. A.; Requena, A. *J. Chem. Phys.* **1980**, *72*, 3018.
- (6) Beswick, J. A.; Requena, A. *J. Chem. Phys.* **1980**, *73*, 4347.
- (7) Halberstadt, N.; Bréchnignac, P.; Beswick, J. A.; Shapiro, M. *J. Chem. Phys.* **1980**, *84*, 170.
- (8) Xiao, Y. S.; Poirier, B. *J. Chem. Phys.* **2005**, *122*, 124318.
- (9) Johnston, R. L. *Atomic and Molecular Clusters*; Taylor and Francis: London, 2002.
- (10) Koperski, J. *Van der Waals Complexes in Supersonic Beams*; Wiley-VCH: Weinheim, 2003.
- (11) Balakrishnan, N.; Forrey, R. C.; Dalgarno, A. *Phys. Rev. Lett.* **1998**, *80*, 3224.
- (12) Forrey, R. C.; Kharchenko, V.; Balakrishnan, N.; Dalgarno, A. *Phys. Rev. A* **1999**, *59*, 2146.
- (13) Boothroyd, A. I.; Martin, P. G.; Peterson, M. R. *J. Chem. Phys.* **2003**, *119*, 3187.
- (14) Kalinin, A.; Kornilov, O.; Rusin, L. Y.; Toennies, J. P. *J. Chem. Phys.* **2004**, *121*, 625.
- (15) Gianturco, F. A.; González-Lezana, T.; Delgado-Barrio, G.; Villareal, P. *J. Chem. Phys.* **2005**, *122*, 084308.
- (16) Li, Y.; Lin, C. D. *J. Phys. B* **1999**, *32*, 4877.
- (17) Poirier, B. *Chem. Phys.* **2005**, *308*, 305.
- (18) Poirier, B. *J. Chem. Phys.* **1998**, *108*, 5216.
- (19) Poirier, B.; Light, J. C. *J. Chem. Phys.* **1999**, *111*, 4869.
- (20) Poirier, B.; Light, J. C. *J. Chem. Phys.* **2001**, *114*, 6562.
- (21) Poirier, B.; Carrington, T., Jr. *J. Chem. Phys.* **2002**, *116*, 1215.
- (22) Bian, W.; Poirier, B. *J. Theor. Comput. Chem.* **2003**, *2*, 583.
- (23) Donley, E. A.; Claussen, N. R.; Thompson, S. T.; Wieman, C. E. *Nature (London)* **2002**, *417*, 529.
- (24) Sutcliffe, B. T.; Tennyson, J. *Int. J. Quantum Chem.* **1991**, *39*, 183.
- (25) Littlejohn, R. G.; Reinsch, M. *Phys. Rev. A* **1995**, *52*, 3035.
- (26) Harris, D. O.; Engerholm, G. G.; Gwinn, W. D. *J. Chem. Phys.* **1965**, *43*, 1515.
- (27) Dickinson, A. S.; Certain, P. R. *J. Chem. Phys.* **1968**, *49*, 4209.
- (28) Light, J. C.; Hamilton, I. P.; Lill, J. V. *J. Chem. Phys.* **1985**, *82*, 1400.
- (29) Colbert, D. T.; Miller, W. H. *J. Chem. Phys.* **1992**, *96*, 1982.
- (30) Szalay, V. *J. Chem. Phys.* **1996**, *105*, 6940.
- (31) Light, J. C.; Carrington, T., Jr. *Adv. Chem. Phys.* **2000**, *114*, 263.
- (32) Littlejohn, R. G.; Cargo, M.; Carrington, T., Jr.; Mitchell, K. A.; Poirier, B. *J. Chem. Phys.* **2002**, *116*, 8691.
- (33) Press, W. H.; Flannery, B. P.; Teukolsky, S. A.; Vetterling, W. T. In *Numerical Recipes*, 1st ed.; Cambridge University Press: Cambridge, England, 1989.
- (34) Montgomery, J.; Poirier, B. *J. Chem. Phys.* **2003**, *119*, 6609.
- (35) Zare, R. N. *Angular Momentum*; John Wiley & Sons: New York, 1988.
- (36) Reinhardt, W. P. *Annu. Rev. Phys. Chem.* **1982**, *33*, 223.
- (37) Jolicard, G.; Austin, E. *J. Chem. Phys.* **1986**, *103*, 295.
- (38) Grozdanov, T. P.; Mandelshtam, V. A.; Taylor, H. S. *J. Chem. Phys.* **1995**, *103*, 7990.
- (39) Seideman, T.; Miller, W. H. *J. Chem. Phys.* **1992**, *96*, 4412.
- (40) Poirier, B.; Carrington, T., Jr. *J. Chem. Phys.* **2003**, *119*, 77.
- (41) Muga, J. G.; Palao, J. P.; Navarro, B.; Egusquiza, I. L. *Phys. Rep.* **2004**, *395*, 357.
- (42) Forrey, R. C.; Balakrishnan, N.; Kharchenko, V.; Dalgarno, A. *Phys. Rev. A* **1998**, *58*, 2645.